CONF-950401--24

Note: This is a preprint of a paper submitted for publication. Contents of this paper should not be quoted or referred to without permission of the author(s).

For publication in *Proceedings of the American Ceramic Society 97th Annual Meeting*, Symposium on The Role of Ceramics in Advanced Electro-Chemical Devices,
Cincinnati, Ohio, April 30–May 3, 1995

THIN-FILM RECHARGEABLE LITHIUM BATTERIES

N. J. Dudney, J. B. Bates, and D. Lubben

Solid State Division
Oak Ridge National Laboratory
Oak Ridge, Tennessee 37831-6030

Prepared by:
SOLID STATE DIVISION
OAK RIDGE NATIONAL LABORATORY
Managed by
LOCKHEED MARTIN ENERGY SYSTEMS
under
Contract No. DE-AC05-84OR21400
with the
U.S. DEPARTMENT OF ENERGY
Oak Ridge, Tennessee

June 1995

THIN-FILM RECHARGEABLE LITHIUM BATTERIES

N. J. Dudney, J. B. Bates, and Dan Lubben
Solid State Division
Oak Ridge National Laboratory
P.O. Box 2008
Oak Ridge, TN 37831-6030

ABSTRACT

Thin-film rechargeable lithium batteries using ceramic electrolyte and cathode materials have been fabricated by physical deposition techniques. The lithium phosphorous oxynitride electrolyte has exceptional electrochemical stability and a good lithium conductivity. The lithium insertion reaction of several different intercalation materials, amorphous V_2O_5, amorphous $LiMn_2O_4$, and crystalline $LiMn_2O_4$ films, have been investigated using the completed cathode/electrolyte/lithium thin-film battery.

INTRODUCTION

Rechargeable thin-film lithium batteries have been fabricated and evaluated at ORNL. These batteries have very high specific energies and power densities, due to the low mass and reactivity of lithium, and are being developed for a variety of small electronic devices including computer memory devices, active transdermal electrodes, and personal hazardous gas sensors.

These rechargeable cells are based on the reversible intercalation or insertion of large amounts of lithium into a transition metal oxide based cathode, $xLi + Li_yMO_z \leftrightarrow Li_{x+y}MO_z$. The free energy of this reaction determines the operating voltage of the battery. The cathode material must be a good mixed conductor and be chemically and physically stable over many cycles of the charge-discharge reaction. The lithium electrolyte separating the lithium anode and the Li_yMO_z cathode should have a high lithium ion conductivity with a transference number of unity, and it must also be stable in contact with both the lithium anode and the cathode at

the voltages of the fully charged battery. Many rechargeable lithium battery systems under development utilize polymer or liquid electrolytes which do not meet these criteria. This restricts the choice of the anode-cathode materials and limits the cycle life of the battery.

A ceramic thin-film lithium phosphorous oxynitride, developed at ORNL in 1991, met the transport and stability requirements for the electrolyte and enabled the fabrication of thin-film batteries with high operating voltage, long term stability and long cycle life [1]. Recent work at ORNL has focused on the fabrication and properties of several thin-film oxide cathode materials. These are very complex ceramic materials for which there is much to be done to understand the chemistry, mass, and charge transport properties. The properties of the thin-film electrolyte and cathode materials are reviewed in this paper.

BATTERY FABRICATION

A cross-section of a typical thin-film cell is shown in Fig. 1. The active area of the batteries fabricated at ORNL ranged from 0.5 to 10 cm^2, with an overall thickness on the order of 10 μm. The simple planar geometry and smooth interfaces make it feasible to evaluate the fundamental thermodynamic properties of the materials and the ion transport rates at each film and interface.

The batteries were fabricated [2] by successive film depositions onto several different insulating substrates, including alumina, glass, and polyester. Current collectors, 0.1–0.5 μm thick, were deposited by dc sputtering of V, Ni, or Pt in Argon. The choice of material depended on the subsequent processing conditions; for example, cathode films annealed at high temperature in oxygen required a Pt current collector. The cathode film, 0.1–4 μm thick, was deposited over the current collector by electron-beam evaporation or magnetron sputtering. The electrolyte, ~1 μm thick, was deposited over an area large enough to completely cover the cathode and to form a protective barrier between the substrate and the lithium anode. Finally a 1-5 μm thick lithium film, deposited from a thermal evaporation source at $<5 \times 10^{-7}$ torr, formed the anode and completed the battery.

Following the lithium deposition, most of the batteries were then sealed in a small Ar-filled glass or stainless steel container with electrical feedthroughs. In some cases, a protective coating was applied to the

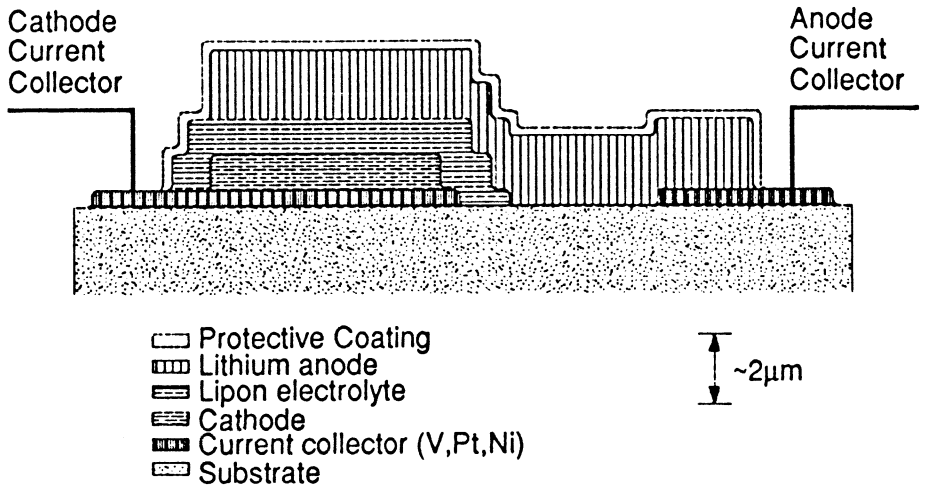

Fig. 1. Cross-section of thin-film battery.

batteries so they could withstand handling in the air. The protective coating consisted of multiple films beginning with either parylene or the electrolyte, which do not react with the lithium anode, then alternating this material with several layers of a metallic or ceramic film to ensure a hermetic barrier.

THIN-FILM ELECTROLYTE

The thin-film electrolyte, referred to as 'Lipon', is an amorphous lithium phosphorous oxynitride material developed at ORNL [1,3]. A typical composition, as determined by Rutherford Backscattering and Proton Induced Gamma Emission, was $Li_{3.3}PO_{3.8}N_{0.24}$; the N content varied up to ~0.46. This material was deposited over the battery cathode at ambient temperatures by rf magnetron sputtering of a Li_3PO_4 target with 20 mTorr N_2 process gas. The 2-inch diameter sintered target was >90% of the theoretical density for Li_3PO_4.

Earlier work on thin films of orthosilicate-orthophosphate compositions produced films with good lithium conductivities [1,4], but these materials proved to be unstable in contact with metallic lithium. As has been shown

in the literature, the substitution of a small amount of nitrogen for some of the oxygen in oxide glasses, including silicates, phosphates and borates, can greatly affect the chemical, mechanical, and thermal stability of the glasses [5]. Likewise with the Lipon thin-films, we found improved stability in contact with lithium, a wider stability window (~5.5 V with respect to Li [6]), and an enhanced lithium ion conductivity compared to the amorphous Li_3PO_4 films.

The measured lithium ion conductivities of several sputter-deposited thin films are shown in Table I. These results showed that the N substitution enhanced the magnitude and reduced the activation energy for the lithium ion conductivity. This may be associated with an increased degree of crosslinking between the phosphate groups in the glass structure due to the N substitution [1]. Attempts to further increase the N content of the films have proven unsuccessful; however , the contribution of a ~1 μm × 1 cm^2 Lipon film to the overall battery resistance is ~20–50 ohms, which has been found to be small compared to the resistance of the cathode film and the cathode/electrolyte interface. The electronic conduction in the Lipon was found to be negligible as batteries stored for >1 year had no significant loss of voltage.

Table I. Composition and Lithium Ion Conductivity of Thin-Film Electrolytes Prepared by rf Magnetron Sputter Deposition.

Composition	Conductivity at 25°C (S/cm)	Activation Energy* (eV)
$Li_{2.7}PO_{3.9}$	7×10^{-8}	0.68
$Li_{3.1}PO_{3.8}N_{0.16}$	200×10^{-8}	0.57
$Li_{3.3}PO_{3.8}N_{0.22}$	240×10^{-8}	0.56
$Li_{2.9}PO_{3.3}N_{0.46}$	330×10^{-8}	0.54
$Li_{3.6}(Si_{0.19}P_{0.81})O_{4.2}$	130×10^{-8}	0.57

*Calculated from least-squares fit of conductivity data to the Arrhenius function, $\sigma T = \sigma_O \exp(-E_a/kT)$.

THIN-FILM CATHODES

Several different intercalation compounds have been prepared and evaluated as the thin-film battery cathode. These include both crystalline

and amorphous $LiMn_2O_4$ films, deposited as the ternary compound, and also amorphous V_2O_5 films, deposited as the lithium-free compound.

Vanadium pentoxide films were deposited by reactive dc magnetron sputtering of a 2-inch V target with a 14% O_2 in Ar process gas mixture at a total pressure of 20 mTorr [2,3]. The film deposition rate was ~0.1 μm/hr and the substrate temperatures did not exceed 50°C during the deposition. The resulting films had a dense microstructure and were amorphous to both x-ray diffraction and electron diffraction. The film density determined from comparison of the measured film deposition rates and profiled film thicknesses was 3 ± 0.1 g/cm^3. Film compositions determined by Auger and RBS spectroscopy were $O/V = 2.5 \pm 0.1$. Sputter deposited crystalline films, on the other hand, had a low density microstructure which proved unsuccessful as a battery cathode due to the poor cathode/electrolyte contact area which resulted in a high cell resistance [3].

Amorphous lithium manganese oxide films were also deposited by magnetron sputtering, in this case using rf power. Films were grown using a 2-inch diameter $LiMn_2O_4$ target, sintered to ~70% of theoretical density, and an 2–10% O_2-Ar gas mixture at 5 mTorr pressure. Although unheated, the film substrates reached ~100°C during the film growth which had a rate of ~0.05 μm/hr. The films were x-ray amorphous and had a density of ~4.2 g/cm^3, approximately that of the crystalline compound. The as-deposited amorphous films were used as the battery cathodes. Samples of these films, which were annealed at 800°C following the deposition, were found to crystallize with the expected spinel structure.

Cathodes of crystalline lithium manganese oxide were formed by a high-temperature anneal of films deposited by electron-beam evaporation techniques [2]. The films were vapor deposited at ambient temperatures with a rate of ~1 μm/hr from a $LiMn_2O_4$ source. The post-deposition anneal was done in a tube furnace under flowing O_2 at 700–800°C for 20 m to 4 h. Examination of the films by SEM microscopy and x-ray diffraction revealed a dense microstructure, submicron grains, and a spinel crystal structure. Precise compositions of the crystalline and amorphous $LiMn_2O_4$ thin films have not been determined; however, the electrochemical results from the Li-cell titrations are consistent with an initial cathode composition near the stoichiometric $LiMn_2O_4$.

CELL TESTS

Cycling characteristics of the completed (Cathode / Lipon / Lithium) cells were determined largely by the properties of the cathode film so this proved to be an excellent way to probe the electrochemical properties of the cathode materials. Cells were cycled using calibrated high-impedance channels of a Maccor battery tester. Most measurements were made at ambient temperatures with selected cells tested at temperatures up to 100°C. AC impedance techniques (0.01–1 MHz) were also used to characterize the cell properties.

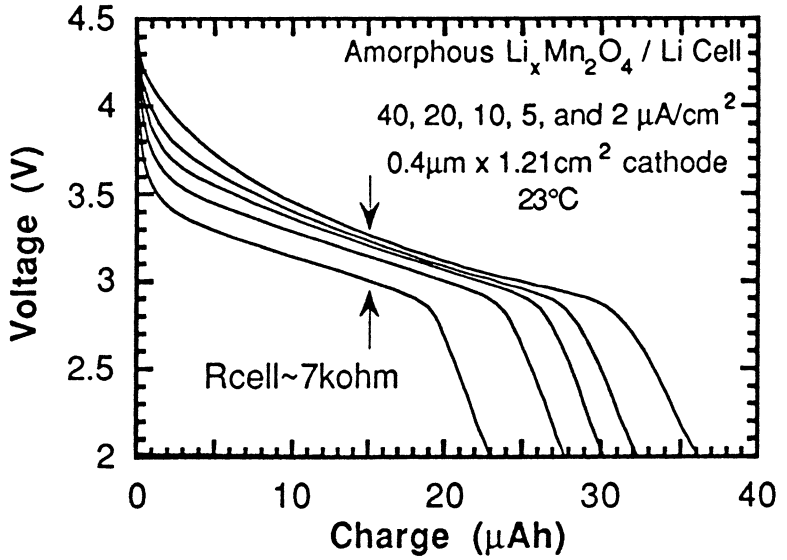

Fig. 2. Discharge curves for a thin-film battery with an amorphous $LiMn_2O_4$ cathode at 40, 20, 10, 5, and 2 $\mu A/cm^2$.

Measurements of the voltage as the cells were discharged at different current densities were used to evaluate the cell resistance. When discharged at higher current densities, the IR loss increased resulting in an incomplete utilization of the cathode capacity. An example is shown in Fig. 2 for an amorphous $LiMn_2O_4$ cathode where the separation of the discharge curves was used to estimate the cell resistance, in this case 7 kΩ. Estimates of the resistance from the discharge curves generally agreed

well with low frequency ac impedance and dc pulse techniques. For some cathodes, the cell resistance varied with the state of charge.

Typical cell resistances estimated from the discharge curves for various cathodes and temperatures are shown in Table II. These are typical of cells fabricated with the optimized processing conditions for each type of cathode as determined to date. Although the properties of each of the cathodes were found to be sensitive to the particular synthesis conditions, these variations will not be discussed here. As illustrated by the tabulated values, it was clear that the cells with the crystalline spinel $LiMn_2O_4$ cathode had a lower resistance than cells with either of the amorphous cathodes. For cells cycled at higher temperatures, the cell resistance was observed to decrease about an order of magnitude. Also, the resistance typically decreased as the cathode thickness was reduced, until the cathode resistance became comparable to the resistance attributed to the cathode-electrolyte and/or cathode-current collector interface.

Table II. Resistance of Thin-Film Batteries as Estimated from the Discharge Curves at Different Current Densities.

Cell Resistance* (kΩ)	Cathode Composition**	Dimensions (μm × cm²)	Substrate
14	a-$Li_xV_2O_5$ 0<x<3	0.13 × 1.21	glass
2	a-$Li_xV_2O_5$ 0<x<3	0.5 × 1.21	alumina
0.3	c-$Li_xMn_2O_4$ 0.5<x<1	0.3 × 1.21	alumina
0.7	c-$Li_xMn_2O_4$ 0.5<x<1	4.0 × 1.0	alumina
7	a-$Li_xMn_2O_4$ 0<x<1	0.44 × 1.21	alumina
0.3 (100°C)	a-$Li_xMn_2O_4$ 0<x<1	0.44 × 1.21	alumina

*At 23°C, unless noted otherwise.
**Amorphous (a) and crystalline (c) cathodes.

Charge-discharge measurements of cells with low current densities, <10 μA/cm², were used to approximate the equilibrium cell potential as lithium was titrated into and out of the cathode film. For the thin-film cells with the Lipon electrolyte, all of the charge transferred was attributed

to motion of the lithium into and out of the cell cathode as there was no indication of corrosion reactions, decomposition of the electrolyte, or charge leaking through the cell. The charge, as μAh, was recorded as the cells were cycled. The specific charge (μAh/mg) or the molar lithium concentration (x) for the cathode was calculated using the cathode area, thickness, determined either by the film profile or the deposition rate, film density and composition. The uncertainties in these calculations were ±5–10%. The low-current charge-discharge curves indicated the ultimate capacity of the cathodes, the compositions associated with phase transitions, and the extent of the irreversible changes in the cathode as the cell was cycled. In some cases, the low-current cycles were insufficient to determine the equilibrium cell potential and true open circuit measurements of the equilibrated cells were therefore recorded.

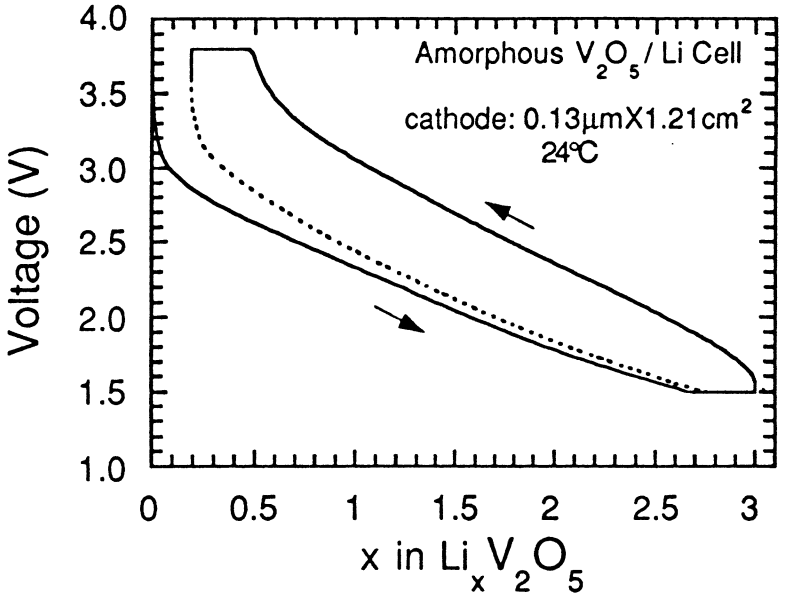

Fig. 3. Initial discharge-charge cycles at 24°C of a thin-film battery with an amorphous V_2O_5 cathode. The battery was cycled 3.8–1.5 V at 10 μA/cm^2, holding at the upper and lower cutoff voltages until the current decayed to 1μA.

Figure 3 shows the first 3 half-cycles for a V_2O_5/Li thin-film cell measured at a low current density [2]. For as-prepared cells with V_2O_5 cathodes

containing no lithium, the open circuit potentials were near 3.4 V. The first discharge to 1.5 V resulted in insertion of 3 moles of lithium into the cathode. Subsequent cycles indicated that at least 2.8 moles of lithium continued to be exchanged at each cycle.

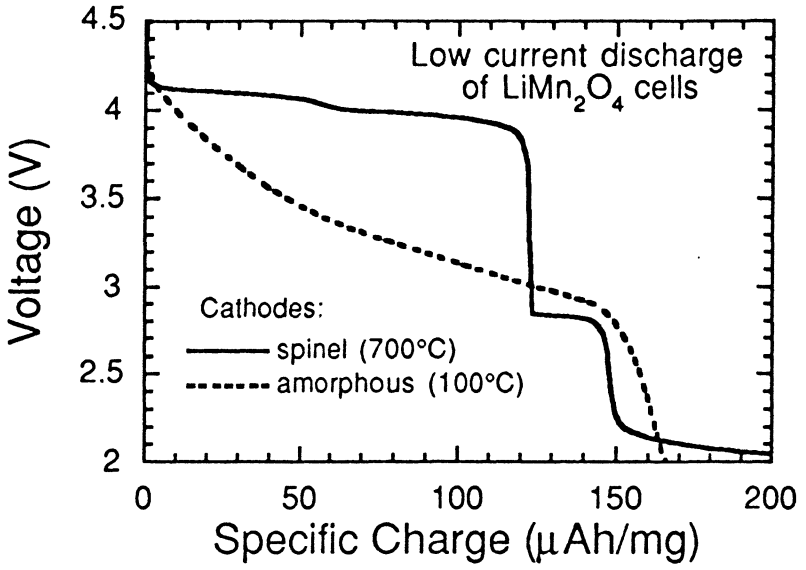

Fig. 4. Low current discharge curves for two thin-film $LiMn_2O_4$ / Li batteries, one with a crystalline spinel cathode annealed at 700°C and one with an amorphous cathode deposited at 100°C. Discharge at 24°C.

Identifying a reference point for the lithium concentration of the $LiMn_2O_4$ cathodes was more difficult because the lithium content of the as-prepared cathode was unanalyzed. Open circuit values for the as-prepared thin film cells varied from 2.8 to near 4 V. Figure 4 shows the low-current discharge of two cells, one with a crystalline spinel cathode and one with an amorphous cathode. From information in the literature for powder compacts of $LiMn_2O_4$ [7,8], a plateau at ~4 V, as observed for the crystalline cathode, corresponds to intercalation of lithium in and out of the tetrahedral lattice sites of the spinel. Alternatively, intercalation of excess lithium ($x>1$) into interstitial sites of the spinel occurs at ~3 V. The

addition of excess lithium in the structure eventually leads to a cubic → tetragonal phase transformation when the average Mn valence becomes 3.5 [7].

For the spinel cathode, the sharp transition from the ~4 V plateau to ~3 V was used as the reference point corresponding to x = 1. The low current discharge-charge data plotted vs. lithium composition is shown in Fig. 5. The high voltage range, 4.5–3.8 V for x<1 of this cathode, was highly reversible and most attractive for the thin-film battery application [2]. The second step in the discharge curve, to ~2 V, was attributed to the cubic → tetragonal phase change. Equilibration in this two-phase region of 1<x<2 was very slow as shown by the large loop formed by the charge-discharge curves around the open circuit measurements. Almost all the lithium was removed from the spinel cathodes when the batteries were charged to 5.3 V, although this led to an irreversible change in the spinel cathode [9].

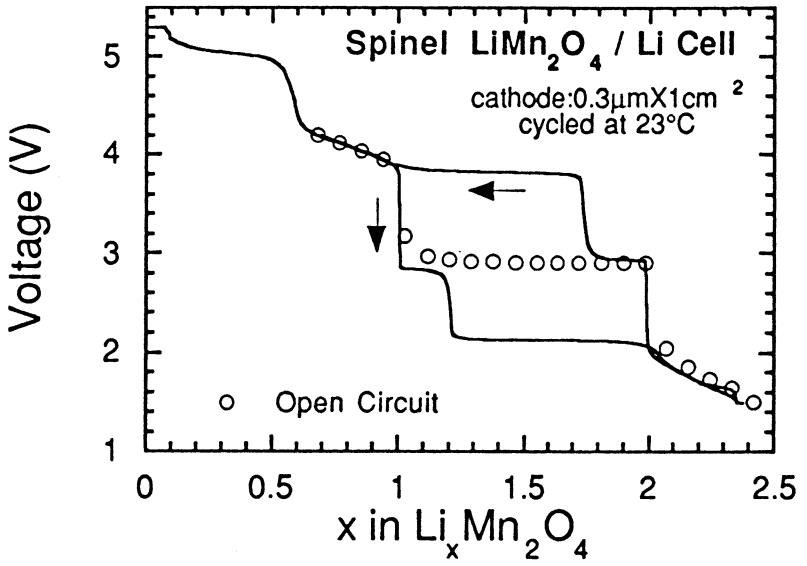

Fig. 5. Low current discharge (4.5 → 1.5 V) and charge (1.5 → 5.3 V) of a lithium battery with a crystalline spinel cathode. Data points are open circuit voltage measurements upon discharge/charge.

A similar plot of voltage versus lithium concentration for a battery with the amorphous $LiMn_2O_4$ cathode is shown in Fig. 6. There were no sharp steps in the discharge curve that could be used as a reference point for the lithium composition; however, assuming x~0 for the battery charged to 4.5 V provided a consistent interpretation of the results. Upon discharge, the voltage decreased smoothly to ~3 V corresponding to the range $0<x<1$. A hysteresis was observed when the cells were cycled between 4.5 and ~3 V, even for the open circuit voltage measurements shown by the open circles. For higher lithium contents $1<x<2$, a step in the discharge curve and a loop between the discharge/charge curves, similar to that of the crystalline spinel cathode, was observed. Presumably, the excess lithium again led to a reversible tetragonal distortion of the local atomic structure. Charging batteries with the amorphous cathode from 4.5 to 5.3 V resulted in little additional charge transfer, which again supported the assumption that x~0 for the amorphous cathode when the cell was charged to 4.5 V.

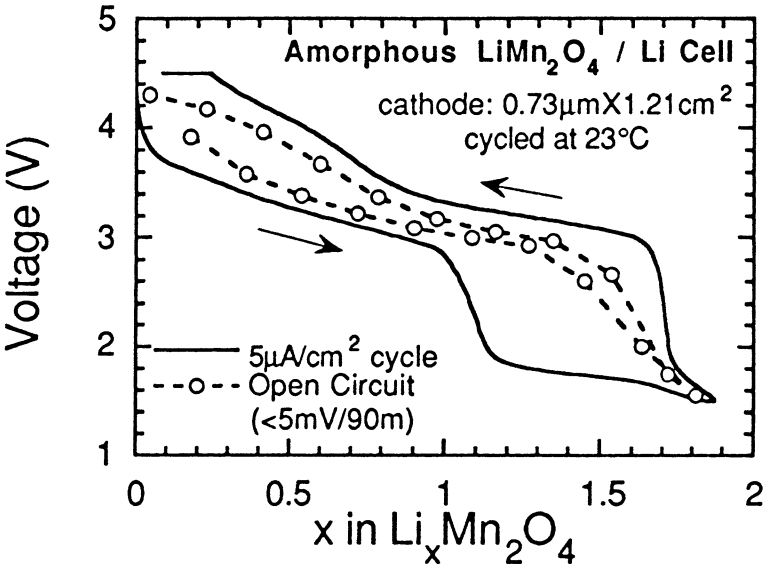

Fig. 6. Low current discharge/charge of a lithium battery with an amorphous $LiMn_2O_4$ cathode (4.5–1.5 V). Open circuit measurements, shown as circles, were recorded when $\Delta V/\Delta t < 3.3$ mV/h for the same discharge/charge cycle.

Battery tests also included long-term cycling. Plots of the measured half-cycle cell capacity as a function of the cycle number, such as shown in Fig. 7, were used to assess the rate of the capacity loss with cycle history, a process common to all rechargeable batteries. The results in Fig. 7 show cycling data at three temperatures. The scatter in the ambient temperature data was due to temperature fluctuations. The specific capacity increased with temperature because of the reduced IR losses at higher temperatures.

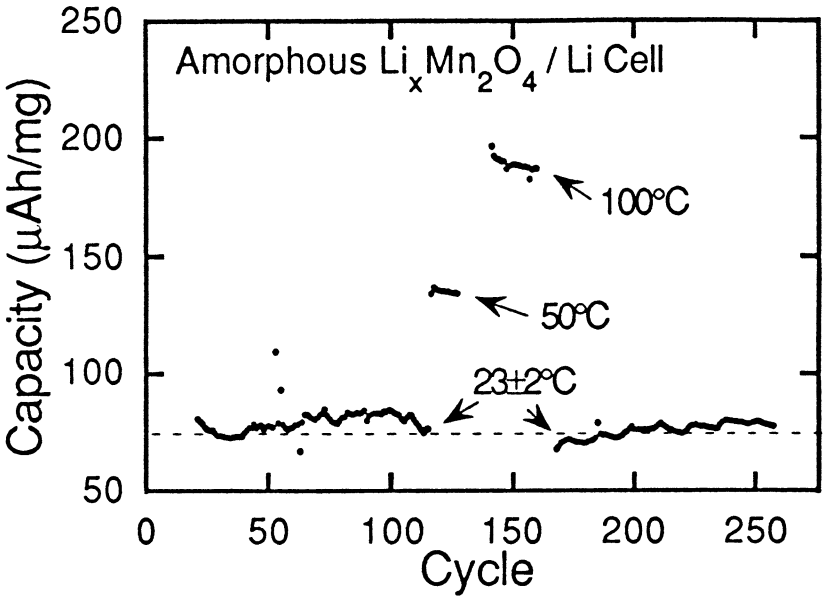

Fig. 7. Discharge capacity upon cycling a thin-film battery with an amorphous $LiMn_2O_4$ cathode (0.44 μm × 1.21 cm^2) and Li anode. A specific capacity of 148 μAh/mg corresponds to 1 mole Li per Mn_2O_4 in the cathode. The battery was cycled at each temperature between 4.5 and 2.0 V at 20 $\mu A/cm^2$.

Generally, the long term cycling results were well represented by a constant fraction capacity loss per cycle, $C = C_O(1-\Delta)^n$. The capacity fade rate, Δ, varied from cell to cell and also depended strongly on the specific cycling conditions. Cycling batteries such that a larger fraction of the cathode capacity was utilized, i.e. over a wider voltage range [2] or at a

lower current density [6], has been associated with a higher rate of capacity loss. For batteries with the spinel cathode, overcharging the cell to >5 V and cycling through the cubic → tetragonal phase transformation, resulted in a significant capacity loss [6,9]. For cells with the V_2O_5 cathode, cycling at 60°C resulted in an enhanced loss rate [2], whereas the higher temperature operation was not as deleterious for the cells with the amorphous $LiMn_2O_4$ cathodes (Fig. 7). Some results of the longer term cycling are listed in Table III. The scatter in the data of Fig. 7 precluded a good fit of the capacity loss rate, but Δ is at least an order of magnitude smaller than that listed in the table for another a-$LiMn_2O_4$ battery. The physical process(es) giving the gradual capacity loss with extended cycling have not been clearly identified and are the subject of ongoing investigations.

Table III. Capacity Loss of Batteries with Different Cathodes and Cycling Conditions.

Cell Cathode	Δ, Fraction Loss Per Cycle	Cathode Dimensions ($\mu m \times cm^2$)	Cycling Conditions V range (V)	Cycling Conditions Current ($\mu A/cm^2$)
a-V_2O_5	1×10^{-3}	0.13×1.21	3.4–1.5	10
c-$LiMn_2O_4$	6×10^{-5}	0.3×1.21	4.5–3.8	20
a-$LiMn_2O_4$	3×10^{-3}	0.74×1.21	4.5–3.0	20

SUMMARY

Thin-film batteries were fabricated and tested. The Lipon electrolyte, developed at ORNL, was shown to be stable in contact with lithium at cathode voltages up to 5.5 V with respect to lithium, and to have a good lithium ion conductivity and a negligible electronic conductivity. Thin-film batteries made with this electrolyte have exceptional shelf- and cycle-life characteristics.

The cycling characteristics of the batteries depended largely on the properties of the cathode film; several different cathode films, amorphous V_2O_5, amorphous $LiMn_2O_4$, and crystalline $LiMn_2O_4$, were investigated. Cells with the amorphous cathodes had a higher resistance than that found for cells with the crystalline $LiMn_2O_4$. The cells with the V_2O_5 cathode, had a particularly high energy density because almost 3 moles of lithium was

cycled reversibly for this cathode. The charge-discharge curves for the $LiMn_2O_4$ cells reflected the different atomic structures and phase transitions as a function of the lithium concentration in the material. The cycle life of the cells depended on the depth of discharge and other factors, but extended cycling results indicated that thousands of cycles could be achieved without excessive loss of capacity for each type of thin film battery.

Characterization of the thin-film batteries has identified a number of challenging problems for future work. For example, the processes resulting in the observed capacity fading, the charge-discharge hysteresis for the amorphous cathodes, and the impeded cubic-tetragonal phase transition for the $LiMn_2O_4$ thin-film cathodes have not been identified. In addition, much remains to be done to characterize the defect chemistry, and charge/mass transport in bulk $LiMn_2O_4$ and other lithium intercalation compounds. There are opportunities for ceramists to contribute to the study of the properties and processing of these ceramic materials for the rechargeable lithium battery technologies.

REFERENCES

[1] J. B. Bates, N. J. Dudney, G. R. Gruzalski, R. A. Zuhr, A. Choudhury, and C. F. Luck, "Electrical Properties of Amorphous Lithium Electrolyte Thin Films," *Solid State Ionics*, **Vol. 53–56**, 647–654 (1992).

[2] J. B. Bates, N. J. Dudney, D. C. Lubben, G. R. Gruzalski, B. S. Kwak, X. Yu, and R. A. Zuhr, "Thin-Film Rechargeable Lithium Batteries," *J. Power Sources* **54 [1]**, 58–62 (1995).

[3] J. B. Bates, N. J. Dudney, G. R. Gruzalski, R. A. Zuhr, A. Choudhury, and C. F. Luck, "Fabrication and Characterization of Amorphous Lithium Electrolyte Thin Films and Rechargeable Thin Film Batteries," *J. Power Sources* **43–44**, 103–110 (1993).

[4] J. B. Bates, N. J. Dudney, C. F. Luck, B. C. Sales, R. A. Zuhr, and J. D. Robertson, "Deposition and Characterization of Li_2O-SiO_2-P_2O_5 Thin Films," *J. Am. Ceram. Soc.* **76 [4]**, 929–943 (1993).

[5] S. Sakka, "Oxynitride Glasses," p. 29–46 in *Annual Review of Materials Science*, Vol. 16, ed. by R. A. Huggins, J. A. Giordmaine, and J. B. Wachtman, Jr., Annual Reviews Inc., Palo Alto, California, 1986.

[6] J. B. Bates, D. Lubben, and N. J. Dudney, "Thin-Film Li-$LiMn_2O_4$ Batteries," *Aerosp. Electron. Syst. Mag.* **10 [4]**, 30 (1995).

[7] R. J. Gummow and M. M. Thackeray, "An Investigation of Spinel-Related and Orthorhombic $LiMnO_2$ Cathodes for Rechargeable Lithium Batteries," *J. Electrochem. Soc.* **141 [5]**, 1178–1182 (1994).

[8] T. Ohzuku, M. Kitagawa, and T. Kirai, "Electrochemistry of Manganese Dioxide in Lithium Nonaqueous Cell. III. X-Ray Diffractional Study on the Reduction of Spinel-Related Manganese Dioxide," *J. Electrochem. Soc.* **137 [3]**, 769–775 (1990).

[9] J. B. Bates, D. Lubben, and N. J. Dudney, "Five-Volt Plateau in $LiMn_2O_4$ Thin Films," *J. Electrochem. Soc.* (in press).

ACKNOWLEDGMENTS

The authors thank Mr. Chris Luck for assistance in fabrication of many of the batteries discussed in this work. This research was sponsored by The Department of Energy's Division of Materials Sciences, Division of Chemical Sciences, Office of Energy Research Technology Transfer Program, and the Office of Transportation Technologies under contract No. DE-AC05-84OR21400 with Lockheed Martin Energy Systems.